FGF8-mediated signaling regulates tooth developmental pace during odontogenesis

Chensheng Lin[1], Ningsheng Ruan[1], Linjun Li[1], Yibin Chen[1], Xiaoxiao Hu[1], YiPing Chen[2], Xuefeng Hu[1]*, Yanding Zhang[1]*

[1]Fujian Key Laboratory of Developmental and Neural Biology & Southern Center for Biomedical Research, College of Life Sciences, Fujian Normal University, Fuzhou, Fujian, 350117, P.R. China.

[2]Department of Cell and Molecular Biology, Tulane University, New Orleans, LA 70118, USA.

Running title: FGF8 regulates tooth developmental pace

***Correspondence to:**

Yanding Zhang, Ph.D.

College of Life Sciences, Fujian Normal University (Qishan Campus), Fuzhou, Fujian, 350117, P.R. China.

Phone: +86-13706963408 (tel); E-mail: ydzhang@fjnu.edu.cn

or

Xuefeng Hu, Ph.D.

College of Life Sciences, Fujian Normal University (Qishan Campus), Fuzhou, Fujian, 350117, P.R. China.

Phone: +86-13055734898 (tel) ; E-mail: bioxfh@fjnu.edu.cn

This manuscript is available as a preprint on non-commercial server bioRxiv: https://doi.org/10.1101/2020.09.16.299388.

Conflicts of interest

The authors declare no conflicts of interest.

Data Availability Statement

All the data are available within the article or its supplementary materials.

Abstract

The developing human and mouse teeth constitute an ideal model system to study the regulatory mechanism underlying organ growth control due to the fact that their teeth share highly conserved and well-characterized developmental processes and their developmental tempo vary notably. In the current study, we manipulated heterogenous recombination between human and mouse dental tissues and demonstrate that the dental mesenchyme dominates the tooth developmental tempo and FGF8 could be a critical player during this developmental process. Forced activation of FGF8 signaling in the dental mesenchyme of mice promoted cell proliferation, prevented cell apoptosis via p38 and perhaps PI3K-Akt intracellular signaling, and impelled the transition of the cell cycle from G1- to S-phase in the tooth germ, resulting in the slowdown of the tooth developmental pace. Our results provide compelling evidence that extrinsic signals can profoundly affect tooth developmental tempo and the dental mesenchymal FGF8 could be a pivotal factor in controlling developmental pace in a non-cell-autonomous manner during mammalian odontogenesis.

Key words: FGF8, tooth, developmental pace, non-cell-autonomous.

Introduction

Although mammals possess an almost identical body plan with morphologically and functionally similar organs and systems, their developmental programs and body sizes vary greatly among different species. The intrinsic developmental programs, together with extracellular signals, control the individual organ size and thus body size [1]. Generally, larger-bodied species own longer gestation lengths with slower developmental tempos to acquire larger body sizes [2,3]. Obviously, developmental tempo and organ size are two closely interrelated variables during individual growth (i.e. embryonic development and postnatal growth) and morphogenesis, both of which must be tightly harmonized to ensure the correct establishment of body plan and therefore are the result of a precisely controlled process.

The mechanisms that regulate organ size have been well investigated in non-mammalian models, particularly in *Drosophila melanogaster*, in which roles of TOR (target of rapamycin), insulin/IGF (insulin-like growth factor), Ras/Raf/MAPK, JNK (c-Jun N-terminal kinase), and Hippo signaling pathways are well defined [4]. In mammals, Hippo and IGF pathways have been evidenced to be involved in controlling organ size [5-10]. Additionally, several conserved families of secreted growth factors, including FGF (fibroblast growth factor), BMP (bone morphogenetic protein), and TGF-β (transforming growth factor-β), are deemed to be involved in the regulation of individual growth due to their ability to modulate cell proliferation and apoptosis during embryonic development [4,11,12]. However, the regulatory mechanisms of developmental pace in mammals are remain largely unknown.

71 Mammalian teeth have long served as a model organ for studying fundamental
72 questions in organ development on the molecular basis [13]. The main features of tooth
73 morphogenesis are conserved in the mammalian lineage [14-16], as they are all formed by
74 sequential and reciprocal interactions between epithelium and mesenchyme and share
75 similar processes during tooth development [15]. Despite these considerable homologies,
76 mammalian dentition undergoes remarkable morphological diversification, displaying
77 great variations not only in tooth shape, number, and size but also in developmental pace
78 [13,15,17-19]. Obviously, the period of tooth development in humans takes about 400 days
79 from the initiation stage at embryonic 6th week to tooth eruption at postnatal 6th month.
80 Whereas, this period in mice takes only about 20 days from the determination of tooth
81 forming sites at E10.5 to tooth eruption at postnatal 10th day [13]. Thus, the human and
82 mouse embryonic tooth provides an ideal model system for investigating the regulatory
83 mechanism underlying the developmental tempo, however, the molecular mechanism that
84 regulates the developmental pace of mammalian teeth remains elusive.

85 It is generally believed that diversified forms of organ morphogenesis (including the
86 developmental tempo) among species are achieved by tinkering conserved signaling
87 pathways instead of proposing novel ones during development [20-22]. The difference in
88 organismal growth rate and organ or body size between humans and mice primarily reflect
89 the difference in cell number rather than the cell size [1]. Many lines of evidence from
90 mouse models demonstrate that numerous growth factors of conserved families, such as
91 FGF, BMP, SHH, and Wnt, have been shown to play critical roles in tooth morphogenesis
92 by regulating cell proliferation, differentiation, and apoptosis during odontogenesis

93 [15,16,21,23-27], suggesting their potential roles in the regulation of the developmental tempo.

94 Here, we provide compelling evidence that it is the dental mesenchyme that dominates

95 tooth developmental tempo in a non-cell-autonomous manner and extrinsic FGF8 may

96 act as a critical factor in controlling this process during odontogenesis.

97 # Materials and methods

98 **Mouse models**

99 *Wnt1-Cre* and *R26R*^{Fgf8} mice were described previously [28,29]. Dental mesenchyme-
100 specifically overexpressed *Fgf8* mice were generated by crossing *Wnt1-Cre* mice with
101 *R26R*^{Fgf8} mice. Mutant embryos were identified by PCR genotyping. All wild-type mice
102 were on the CD-1 background. Mice were housed under the following identical conditions:
103 40-70% relative humidity, 12 hour light/dark cycle, and 20-25°C ambient temperature, in
104 individually ventilated cages, with corncob granules for bedding and nesting, in groups
105 of up to six. The mice were given free access to tap water and standard rodent chow
106 (1010011; Jiangsu Xietong Pharmaceutical Bio-engineering Co., Ltd, Nanjing, China).

107 **Tissue recombination, organ culture, and subrenal culture**

108 Fresh lower jaws isolated from human fetuses of 14th-16th week gestation following
109 medical termination of pregnancy were provided by Maternal and Child Health Hospital
110 of Fujian Province, China. The precise embryonic age of fetuses was defined by the
111 measurement of the crown-rump length (CRL) [30]. Human and E13.5 mouse embryonic
112 tooth germs were dissected out in ice-cold PBS and then treated with Dispase II at 37°C
113 for 20 min. The dental mesenchyme and dental epithelium were separated with the aid of
114 fine forceps and incubated on ice for further tissue recombination experiments. Three
115 types of tissue recombination were conducted and are summarized in Table 1: E13.5
116 mouse dental epithelium with bell-stage human dental mesenchyme (14-16 weeks of
117 gestation) (referred to as mde+hdm); E13.5 mouse dental mesenchyme with bell-stage
118 human dental epithelium (hde+mdm); and E13.5 mouse dental mesenchyme with mouse

119 dental epithelium from the same stage as control (mde+mdm). All recombinants were
120 cultured in the Trowell-type organ culture dish overnight, followed by subrenal grafting
121 in adult nude mice, as described previously [30,31]. The use of animals and human tissues
122 in this study was approved by the Ethics Committee of Fujian Normal University
123 (permission #2011005).

124 **SU5402 injection**

125 Two first mandibular premolar germs dissected out from the lower jaw of a human
126 fetus of 16th week gestation were cultured under the kidney capsules of two nude mice,
127 one germ each. SU5402 (Calbiochem, California, USA) and DMSO (Merck, Darmstadt,
128 Germany) was intraperitoneally injected into each recipient mouse at a dose of
129 25mg/Kg/d in 200 μL PBS twice a day for one week. The human tooth grafts were
130 harvested for histological analysis after another week in subrenal culture.

131 **Lentivirus infection and cell re-aggregation**

132 For efficient infection of lentivirus [32], isolated E13.5 mouse dental mesenchyme
133 was digested with 0.25% trypsin at 37 °C for 5 min and dispersed into a single-cell
134 suspension with the aid of a micropipette. To make a dental mesenchyme pellet, about
135 5×10^5 dental mesenchymal cells were infected with 20 μL concentrated lentivirus in 200
136 μL culture medium in an Eppendorf tube. The tube was incubated at 37°C in a 5% CO_2
137 environment for 2 hours with its cap open, centrifuged at 3000 rpm for 3 min, and then
138 incubated again in the same environment for 2 hours. Cell pellets were removed from the
139 tubes, recombined with E13.5 dental epithelium, and cultured in the Trowell-type organ
140 culture dish overnight. Recombinants were subsequently subjected to subrenal culture in

141 nude mice.

142 **Histology, *in situ* hybridization, immunostaining, and Western blot**

143 For histological analysis, harvested samples were fixed in 4% paraformaldehyde
144 (PFA)/PBS, dehydrated, embedded in paraffin, and sectioned at 7 μm. Standard
145 Hematoxylin/Eosin (H&E) and Azan dichromic staining were utilized for histological
146 analysis [33]. Ossified tissues or grafts were demineralized with EDTA/PBS for a week
147 prior to dehydration. For *in situ* hybridization, dental tissues from staged human embryos
148 were dissected out in ice-cold PBS and fixed in 4% RNase-free PFA/PBS at 4°C overnight.
149 Human cDNAs, including *FGF1* (MHS6278-202758608), *FGF2* (EHS1001-208062206),
150 *FGF15/19* (MHS6278-202756089), *FGF18* (MHS6278-202830446), were purchased
151 from Open Biosystems (Alabama, USA) and were subcloned to pBluescript-KS plus
152 vector for riboprobe transcription. Whole-mount *in situ* hybridization and section *in situ*
153 hybridization were performed following standard protocols as described previously [34,35].
154 Immunostaining was performed as described previously [36]. The following primary
155 antibodies were used including the products of Santa Cruz Biotechnology (Texas, USA):
156 Ameloblastin, MMP20, DSP, K-Ras, FGF8, P21; ABCam: FGF4, FGF9, Caspase3,
157 Ccnd1; Cell Signaling Tech (Massachusetts, USA): pSmad1/5/8, pP38, pErk1/2, pJNK,
158 pAKT1, pPDK1; Merck Millipore: β-catenin; and Spring Bio: Ki67. Alexa Fluor 488 or
159 594 IgG (H+L) antibody (Thermo Fisher, Massachusetts, USA) and horseradish
160 peroxidase-coupled IgG antibody (Santa Cruz) were used as the secondary antibody. For
161 immunoblotting, pP38, pErk1/2, pJNK, pAkt, and Actin (Santa Cruz) were used as
162 primary antibodies. IRDye 800cw or 680cw IgG (Odyssey, Nebraska, USA) were used

163 as secondary antibodies. Immunoblotting was conducted as described previously [37].
164 Signals were observed using microscope (Olympus BX51, Tokyo, Japan), Laser scanning
165 confocal microscope (Zeiss LSM780, Jena, Germany), and Infrared Imaging Systems
166 (Odyssey Clx). Representative images were taken from a minimum of 3 replicate
167 experiments.

168 **Micro-computed tomography imaging and analysis**

169 Harvested mineralized teeth were scanned with X-ray micro-computed tomography
170 (microCT) equipment (μCT50, SCANCO Medical AG, Bruettisellen, Switzerland). The
171 microCT parameters were as follows: 19 × 19 mm-field of view, 15-μm voxel size, 70
172 kVp, 200 mA, 360° rotation, 1500ms exposure time. All datasets were exported in the
173 DICOM format with the isotropic 15-μm^3 voxel. Acquired height and width of the tooth
174 crown were analyzed with the attached software of μCT50.

175 **Statistics analysis**

176 Image J software (version 1.46r; National Institutes of Health, USA) was utilized for
177 Ki67-positive cell counting and to detect the densitometry of the western blot bands with
178 at least three biological replicates counted. Statistical analyses were performed with
179 GraphPad Prism 5 (Version 5.01; GraphPad Software Inc, California, USA). Data were
180 represented as mean ± SD. Paired *t*-test was used to evaluate differences between two
181 groups, and analysis of variance (ANOVA) was used to determine differences among
182 different groups. If there was a significance of ANOVA test, Bonferroni post-tests was
183 used. p values <0.05 is considered statistically significant difference.

184 # Results

185 **Tooth developmental pace is dominated by the dental mesenchyme in humans and**
186 **mice.**

187 Our previous studies have shown that epithelial sheets of human keratinocyte stem
188 cells, when recombined with E13.5 mouse dental mesenchyme, can be induced to
189 differentiate into enamel-secreting ameloblasts in only 10 days and apoptotically
190 degraded in 4 weeks, whereas the mouse secondary branchial arch epithelium, when
191 recombined with the human dental mesenchyme from the bell-stage, remains in an
192 enamel-secreting status after 15-week *ex vivo* culture [30,38,39]. These results strongly imply
193 that the duration of epithelial differentiation in tooth development could be dominated by
194 the mesenchymal component in humans and mice. To validate our hypothesis, we
195 comprehensively revisited these phenotypes by carrying out meticulously designed
196 heterogenous recombination between human and mouse embryonic dental tissues (Table
197 1). As shown in Fig. 1A-C, it took more than 4 weeks for the mouse dental epithelium to
198 deposit enamel when recombined with the human dental mesenchyme in mde+hdm
199 chimeric tooth germs and the chimera generated a mineralized tooth after 16-week growth
200 (Suppl. Fig. 1A), exhibiting a much longer developmental duration and slower tempo in
201 comparison with the mouse dental epithelia that were combined with their own dental
202 mesenchyme (Fig. 1D-F, Suppl. Fig. 1B). By contrast, it took only about 10 days for the
203 human dental epithelium to deposit enamel when recombined with E13.5 mouse dental
204 mesenchyme in hde+mdm chimeric tooth germs (Fig. 1G-I) and the chimera could
205 achieve a mineralized tooth in less than 30 days as well as the mouse homogenous

206 (mde+mdm) tooth (Suppl. Fig. 1C), demonstrating a dramatically accelerated
207 developmental pace compared to the normal human tooth morphogenesis.
208 Immunostaining of two ameloblastic differentiation markers, ameloblastin and MMP20
209 (Matrix Metallopeptidase 20), further confirmed the development phase alteration of the
210 dental epithelium induced by the heterogenous dental mesenchyme. The expression of
211 these two markers in the mouse dental epithelium-derived pre-ameloblasts in mde+hdm
212 chimeric recombinants was delayed to 4th week in subrenal culture (Fig. 1J-L), whereas
213 the expression of the two markers was antedated at 9-day in the human dental epithelium-
214 derived ameloblasts in hde+mdm chimeric recombinants in subrenal culture (Fig. 1P-R),
215 which is similar to the expression of them at 7-day in the ameloblasts derived from the
216 mouse dental epithelium in mde+mdm control recombinants (Fig. 1M-O). The possibility
217 of tissue contamination was ruled out using specific primary antibodies against mouse or
218 human MHC I antigens to distinguish between human and mouse tissues in the
219 heterogenous chimeras (Suppl. Fig. 2). Our results unambiguously indicate that the dental
220 mesenchyme is a crucial component that dominates the tooth developmental pace by
221 interaction with the dental epithelium via diffusible paracrine signals during
222 odontogenesis.

223 **FGF signaling participates in the regulation of tooth developmental pace.**

224 We next attempted to identify the paracrine signaling molecules that may be
225 involved in the regulation of tooth developmental tempo in humans and mice. Conserved
226 SHH, FGF, BMP, and Wnt pathways are all crucial signaling engaged in cell proliferation,
227 apoptosis and differentiation during odontogenesis, indicating that they may be key

228 players in orchestrating the fundamental mainspring of organ growth. Since the dental
229 mesenchyme is dominant in the regulation of tooth growth (Fig. 1), we exclude
230 epithelially expressed SHH [40]. To test whether mesenchymal BMP, FGF and WNT
231 signaling may be involved in the regulation of tooth developmental pace, we examined
232 the level of the active indicators of these pathway including pSmad1/5/8 for BMP, K-Ras
233 for FGF, and β-catenin for Wnt, respectively, in the chimeric tooth germs. The expression
234 level of K-Ras in both the dental epithelium and mesenchyme is much higher in the
235 mde+hdm chimeric tooth germ (Fig. 2E), where the development of mouse dental
236 epithelium-derived ameloblasts were dramatically delayed and remained immature after
237 4 weeks in subrenal culture, compared to that in the mouse homogenous recombinant
238 tooth germ (Fig. 2B). The expression levels of pSmad1/5/8 and β-catenin in mouse dental
239 epithelium-derived ameloblasts and adjacently interacted odontoblasts did not display
240 obvious difference as compared between the heterogenous recombinants and
241 homogenous ones (Fig. 2A,C,D,F). The enhanced epithelial FGF activity in the mde+hdm
242 chimeric tooth germ, evidenced by outstandingly enhanced activity of K-Ras, was
243 certainly induced by the human dental mesenchyme and may attribute to the protracted
244 differentiation of the mouse dental epithelium.

245 To explore whether the upregulated FGF signaling may be associated with the
246 prolonged tooth development phase in humans, we started with a search for candidate
247 FGFs that are persistently expressed in the human developing dental mesenchyme but
248 barely in the mouse one. Most expression patterns of 22 known FGF ligands in mammals
249 have been verified in mouse tooth germs at the cap and bell stages (summarized in Suppl.

250 Table 1)[41,42]. We have examined in our previous studies the expression patterns of *FGF3,*
251 *FGF4, FGF7, FGF8, FGF9,* and *FGF10* in human tooth germs at different stages using
252 *in situ* hybridization or immunohistochemistry [43]. Here, we screened the expression of
253 additional 12 *FGFs* that have not been identified in human tooth germs by RT-PCR. We
254 excluded *FGF11, FGF12, FGF13,* and *FGF14*, because they are not secreting ligands
255 and do not activate FGF receptors as well. We found that, among them, the transcripts of
256 *FGF1*, *FGF2*, *FGF15/19*, and *FGF18* were detectable at both the cap and bell stages
257 (data not shown). We further confirmed their expression in developing human teeth by
258 section *in situ* hybridization (Suppl. Fig. 3). When comparing the FGF expression data
259 between the human [43] and mouse [41,42], we noticed that the majority of FGF transcripts
260 are broadly distributed in the whole tooth germ including the dental epithelium and
261 mesenchyme throughout the early cap stage to the late bell stage in humans [43]. However,
262 their expression is restricted to the limited region of tooth germs, such as enamel knot,
263 and appeared in limited periods of time in mice (Suppl. Table 1)[41,42]. We believe that this
264 widely and persistently distributing pattern of FGF ligands in the human tooth germs is
265 closely related to their characteristics of tooth development. To further verify this notion,
266 we cultured human 1st premolar germs at the early bell stage under the kidney capsule of
267 nude mice with intraperitoneal injection of SU5402, a global FGF-signaling inhibitor (an
268 inhibitor of tyrosine phosphorylation of FGF receptor). The inhibition activity of SU5402
269 in human tooth germs was firstly evaluated after two days injection and showed that it
270 significantly inhibited FGF-mediated activation of FGFR downstream signal transduction,
271 pErk1/2 and pPDK1 (Fig. 2G). Then, we cultured the human molar germs with SU5402

272 for one week and found accelerated detinogenesis in the SU5402-treated molar germ with
273 the appearance of both predentin and dentin (Fig. 2I), as compared to DMSO-treated one
274 with appearance of only predentin (Fig. 2H), indicating pivotal roles of FGF-signaling in
275 regulation of tooth developmental tempo.

276 With further analyses of FGF expression data in humans and mice, we found that
277 FGF4, FGF8, and FGF9 ligands exhibit most distinctive patterns (Suppl. Table 1). These
278 three ligands are persistently expressed in the dental epithelium and mesenchyme at least
279 until the differentiation stage in humans [43]. However, in mice, the expression of FGF4 is
280 restricted to the enamel knot from the cap to bell stage and that of FGF9 to the enamel
281 knot at the cap stage and to the dental epithelium at the bell stage. Furthermore, FGF8 is
282 only expressed in the presumptive dental epithelium prior to and during the laminar stage
283 and is no longer expressed after the E12 bud stage [44]. Whereas, in humans, *FGF8*
284 transcripts are widely and intensively present in the whole tooth germ at least from the
285 early cap stage to the differentiation stage [43]. Importantly, we found retained expression
286 of FGF8, as well as FGF4 and FGF9, in the mouse dental epithelium derived pre-
287 ameloblasts in mde+hdm recombinants after 4 weeks in subrenal culture, where the
288 development of mouse ameloblasts was largely delayed (Fig. 2J-L), whereas FGF8 was
289 attenuated in the human dental epithelium derived pre-ameloblasts in hde+mdm
290 recombinants after 10 days in subrenal culture, where the development of human
291 ameloblasts was vastly accelerated (insert in Fig. 2K). Based on these observations, we
292 hypothesized that FGF signaling may play important roles and FGF8 could be a critical
293 factor in the regulation of tooth developmental pace.

294 **Forced activation of FGF8 signaling in the mouse dental mesenchyme delays tooth**
295 **development.**

296 To test our hypothesis, we set to overexpress *Fgf8* in dental mesenchymal cells in
297 the E13.5 recombinant molar germ via lentivirus-mediated expression and subrenal
298 culture system. Histological examination revealed that it took up to 9 days for *Fgf8*-
299 overexpressed tooth grafts to start dentin secreting (Fig. 3B), whereas it only took 7 days
300 for control ones to do so (Fig. 3A). Moreover, Ki67 staining detected remarkably higher
301 level of proliferation rate in both the dental epithelium and mesenchyme of *Fgf8*-
302 overexpressed tooth grafts compared to the controls after 7 days in subrenal culture (Fig.
303 3C-E; *n*=6/group). These data indicate that activated mesenchymal FGF8 activity delays
304 tooth development and dramatically stimulates cell proliferation.

305 To corroborate the aforementioned *ex vivo* results, we further generated *Wnt1-Cre;*
306 $R26R^{Fgf8}$ transgenic mice to verify whether forced activation of mesenchymal FGF8
307 signaling alters tooth development *in vivo*. The presence of FGF8 in the dental
308 mesenchyme of *Wnt1-Cre;*$R26R^{Fgf8}$ mice was confirmed by anti-FGF8 immunostaining
309 (Suppl. Fig. 4). Most of mutant embryos die at around E12.5 and a few died around E14.5.
310 Although histological examination revealed severe craniofacial hypoplasia in 100% cases,
311 including exencephaly and the absence of identifiable tissues such as ears, auricles, eyes,
312 nose, as well as tongue (data not shown), the mutant mice still possessed a pair of intact
313 maxillary and mandibular molar germs (Fig. 4). More importantly, both the maxillary and
314 mandibular molar germ exhibited an obvious retardation of tooth development (Fig. 4).
315 Since most mutant embryos died at around E12.5, we grafted E11.5 mutant molar germs

316 under the kidney capsule for further development. Examination of histology and the
317 deposition of dentin and enamel showed that the mutant maxillary molar developed with
318 approximate one-day's delay when compared to the wild-type ones in nearly 100% (15/16,
319 Fig. 5A-F), and the mutant mandibular molar developed with about two-day's delay in 2
320 out of 9 grafts with the rest 7 failing to develop (insert in Fig. 5D). Examination of the
321 expression of odontoblast marker DSP and ameloblast marker ameloblastin in the grafted
322 maxillary molars further confirmed this delay (Fig. 5I-L).

323 Interestingly, Azan staining showed that the mutant graft of maxillary molar germ
324 formed a larger-sized tooth (Fig. 5G) than the wild-type one (Fig. 5H) after 18 days in
325 subrenal culture. Further Micro-CT scanning revealed that the mutant graft indeed formed
326 a larger-sized tooth with short and dumpy shape (Fig 5N) compared to the control (Fig.
327 5M) after 3 months in subrenal culture for complete mineralization, which exhibited no
328 difference in the average height of the tooth crowns but about 20% wider in the average
329 width in the mutants (n = 11) compared to the controls (n = 7, Fig. 5O). Apparently, higher
330 rate of cell proliferation contributes greatly to the larger teeth, which was evidenced by
331 more Ki67 positive cells presented in E13.5 mutant tooth germ and the grafted mutant
332 teeth than controls (Fig. 6A-F, K-M, n = 3/each group). Meanwhile, while apoptotic
333 marker Caspase3 staining was present in ameloblasts and odontoblasts in both mutant
334 (Fig. 6I,J) and wild-type tooth germs (Fig. 6G,H), this apoptotic signal was non-
335 detectable in the pulp cells of mutant tooth germs (Fig. 6I,J), whereas it was seen in that
336 of wild-type ones (Fig. 6G,H) after 18 days in subrenal culture. These results further
337 support the idea that ectopically activated FGF8 signaling in the mouse dental

338 mesenchyme stimulates cell proliferation and prevents cell apoptosis during
339 odontogenesis.

340 **Ectopically activated dental mesenchymal FGF8 signaling is transduced via p38 and**
341 **PI3K-Akt intracellular pathway.**

342 To determine which intracellular pathway is implicated in the signal transduction of
343 the ectopically activated dental mesenchymal FGF8 signals, we examined the levels of
344 phosphorylated Erk1/2, P38, JNK, and PI3K-Akt, the activity indicator of MAPK
345 pathway, in both E13.5 tooth germs and E11.5 ones after 9 days in subrenal culture. As
346 shown in Fig. 7, no signal intensity differences in pErk1/2 (Fig. 7A-D) and pJNK (Fig.
347 7E-H) staining were observed between wild-type and mutant teeth. Whereas, p38
348 signaling is dramatically elevated in *Wnt1-Cre;R26R*^{Fgf8} teeth with a considerably
349 increased amount of nuclear-localized pP38 cells both in the dental epithelium and dental
350 mesenchyme of E13.5 mutant tooth germs (Fig. 7J) and grafted teeth (Fig. 7L) as
351 compared to the controls (Fig. 7I,K). Meanwhile, the intensity of PI3K-Akt staining was
352 slightly enhanced and the amount of pAkt1^{+} cells was increased in mutant E13.5 tooth
353 germs and grafted teeth (Fig. 7N,P) as compared to controls (Fig7 M,O). Western blot
354 analysis further confirmed the increased expression of pP38 and pAkt1 in E13.5 mutant
355 tooth germs (Fig. 7Q,R; n = 3). Our results indicate that the augmented dental
356 mesenchymal FGF8 activity enhances P38 and PI3K-Akt signaling in both the dental
357 mesenchyme and the dental epithelium, suggesting that they may function as intracellular
358 pathways for transducing FGF8 signal into nuclei.

359 **Enhanced dental mesenchymal FGF8 signaling promotes transition of cell cycle**
360 **from G1- to S-stage during odontogenesis.**

361 The rate of cell proliferation controlled by cell cycle progression is a key player in
362 organ size control [4] and is also closely associated with tissue differentiation status, as
363 higher cell proliferation always presents in developing tissues and lower one in
364 differentiated ones. Since the elevation of *Fgf8* expression in the dental mesenchyme
365 results in the significant promotion of cell proliferation and prevention of cell apoptosis
366 (Fig. 6), we speculated that enhanced dental mesenchymal FGF8 signaling would alter
367 cell cycling. To verify this hypothesis, we set forth to ascertain the distribution of cyclin
368 D1 (Ccnd1) and its inhibitor $p21^{Cip1}$ (p21), a pair of critical regulators functioning
369 stimulatory and repression effect, respectively, on inducing cell cycle entry and mediating
370 the G1-S stage transition [45,46], in E13.5 tooth germs and grafted teeth. As shown in Fig.
371 8, although the same high density of $Ccnd1^+$ cells were present in the dental epithelium
372 of E13.5 wild-type and mutant tooth germs, the dental mesenchyme in mutant tooth germs
373 possessed a considerably increased amount of $Ccnd1^+$ cells in comparison to that in wild-
374 type ones (Fig. 8A,E). On the other hand, $p21^+$ cells were abundantly present in the
375 presumptive primary enamel knot of the dental epithelium and slightly in the dental
376 mesenchyme in wild-type tooth germs but totally absent from the whole tooth germ in
377 mutant ones (Fig. 8B,F). Thereout, more colocalization of Ccnd1 and p21 staining were
378 found in the wild-type tooth germs than in the mutant ones (Fig. 8C-D, G-H). In grafted
379 teeth, nuclear $Ccnd1^+$ cells were distributed not only in ameloblasts and odontoblasts (Fig.
380 8M,P-upper) but also all over the dental pulp in mutants (Fig. 8M,P-lower), rather than

381 being restricted to the dental mesenchymal cells adjacent to the odontoblasts in wild-types
382 (Fig. 8I,L). Although p21 was expressed in ameloblasts and dental mesenchymal cells in
383 both wild-type and mutant teeth, its expression level was relatively decreased in mutants
384 (Fig. 8J,L,N,P). In addition, the nuclear localization of p21 could be detected in dental
385 mesenchymal cells of wild-type teeth (Fig. 8L-lower), whereas it was found to be in the
386 cytoplasm of grafted mutant teeth (Fig. 8P-lower), which make it unable to cooperate
387 with nuclear Ccnd1 to regulate the cell cycle progression in the dental mesenchymal cells.
388 Taken together, these results provide evidence that enhanced mesenchymal FGF8 activity
389 observably elevates the activity of nuclear Ccnd1 while degrades the activity of nuclear
390 p21. Thus both stimulation of Ccnd1 and repression of p21 function to induce cell cycle
391 entry and promote the transition of cell cycle from G1- to S- stage, which facilitates cell
392 population to retain the high rate of proliferation.

393 # Discussion

394 **Tooth developmental tempo complies with the hereditary nature of dental**
395 **mesenchyme.**

396 A heterogenous recombination study carried out between the mouse and rat molar
397 tooth germs has suggested that tooth size is determined by the dental mesenchyme [47,48].
398 Additionally, our recent studies showed that, in comparison with natural developmental
399 pace, the differentiation duration of the mouse dental epithelium or non-dental epithelium
400 into ameloblasts when induced by the human dental mesenchyme is significantly
401 extended, whereas that of the human dental epithelium or epithelial stem cells into
402 ameloblasts when induced by the mouse dental mesenchyme is significantly shortened
403 [38,39]. These results are consistent with the difference of development progression speed
404 between human and mouse teeth [13], suggesting a dominant role of the dental
405 mesenchyme in regulation of tooth developmental tempo. This idea is further supported
406 by our current heterogenous recombination study carried out between the mouse and
407 human molar tooth germs (Fig. 1). We further provide unambiguous evidence that not
408 only the tooth size but also the tooth developmental pace are obedient to the hereditary
409 character of dental mesenchyme.

410 **Dental mesenchymal FGF8 and synergistic effects of FGFs play critical roles in**
411 **controlling the developmental tempo during mammalian odontogenesis**

412 Conserved pathways, such as FGF, BMP, Hh, and WNT pathway, participate in the
413 highly conserved molecular mechanism underlying organismal growth by corresponding
414 alterations of cell growth and division [4,11,12]. FGFs, as the most common mitogens, are

415 positively correlated to the rate of cell growth and cell division and involved in the
416 induction and pattern formation during tooth development [49,50]. Fgf8 has been
417 demonstrated to play an important role in cell survival and proliferation of CNC cells [51],
418 and to exert a positive effect on proliferation of dental mesenchymal cells [44]. Our data
419 show that FGF signaling rather than BMP and WNT signaling is highly active in human-
420 mouse chimeric tooth germs where the differentiation duration of the mouse dental
421 epithelium is largely slowed down (Fig. 2), which is consistent with the continuously high
422 expression of FGFs, particularly FGF8, in human tooth germs, suggesting a potentially
423 positive role of FGF signaling in regulating the tooth developmental tempo during
424 odontogenesis in humans. Both our *ex vivo* lentivirus-mediated overexpression system
425 and *in vivo* transgenic mouse model support that forcibly activated dental mesenchymal
426 FGF8 signaling stimulates cell proliferation and inhibits cell apoptosis, thus prolonging
427 tooth developmental pace in mice (Fig. 3-6). FGF8 appears to be a critical factor in
428 regulating the tooth developmental pace during mammalian odontogenesis.

429 Functional redundancy complicates interpretation of FGF genetic studies.
430 Phenotypes in various *Fgfr* knockout mice have demonstrated that different FGF
431 receptors have both essential and redundant roles throughout development [49]. During
432 odontogenesis, FGF7 and FGF10 have been proven to act as surrogates of mesenchymal
433 FGF3 [52], and FGF4, FGF8, as well as FGF9 have also been suggested functional
434 redundancy and repetitive use in mouse tooth development [13]. Our previous and current
435 study show that several FGFs, especially FGF4, FGF8, and FGF9, have a broad and
436 persistent expression in the whole tooth germs in humans but are restricted to the limited

437 region of tooth germs in mice (Suppl. Table 1) [43]. These data suggest that tooth
438 developmental pace may be the product of synergistic effects of different FGFs in
439 mammals. Actually, in addition to the fact that FGF8 is a key factor to control tooth
440 developmental pace discovered in the current study, Fgf9 has also been reported to induce
441 cell proliferation in cultured mouse dental mesenchyme *in vitro* [44] as well as in cervical
442 loop development *in vivo* [53] and the *Fgf9* null mutant mice show a size-reduced labial
443 cervical loop [53], and FGF4 stimulates cell proliferation in both the dental epithelium and
444 mesenchyme as well [44,54], both suggesting their positive function on the regulation of
445 tooth growth. We speculate that, in humans, several broadly, intensively, and persistently
446 expressed FGF ligands may act in concert to confer growth capability (stimulation of
447 proliferation and prevention of apoptosis) on tooth tissues to achieve longer development
448 time-scale.

449 **FGF pathway may also participate in the regulation of tooth size.**

450 On the other hand, the developmental tempo and size of individual organs must be
451 tightly coordinated to match the body size and larger-bodied species always keep slower
452 developmental tempos to acquire larger organ sizes. Hippo signaling is the only admitted
453 pathway that plays its best-known physiological function on the control of organ size in
454 the mouse model for mammalian lineage [5-8], which mainly involves in the regulation of
455 cell proliferation and apoptosis and thereby cell number [9]. Activation or inhibition of
456 YAP/TAZ, a transcriptional co-activator of Hippo pathway, leads to the adjustment of cell
457 proliferation and apoptosis, thus affecting organ sizes and tissue homeostasis [5-8].
458 However, in tooth development, suppression of YAP *ex vivo* at the cap stage only leads

459 to ectopic cusp formation [55], while overexpression of YAP *in vivo* disrupts tooth
460 morphogenesis with abnormal enamel knot as well as greatly widened dental lamina;
461 teeth ultimately formed in YAP transgenic mice do not exhibit any growth delay or size
462 enlargement [6]. These data suggest that the renowned control function of Hippo pathway
463 in mammalian organ size is not applicable for the tooth organ. In support of this notion,
464 it has also been reported that size-control mechanisms differ across mammalian organs
465 [11] and enhanced Hippo signaling induces organ enlargements in the stomach, heart, liver,
466 and spleen, but not in lung, kidney, and intestine [56-58]. Besides, IGF signaling is the other
467 pathway that has been implied to have effects on organ size and *Igf2r* disrupted mice are
468 born 25-35% bigger than wild-types, however, it has also been revealed that IGF signaling
469 affects the size in some organs such as the cecum and colon but not the size of other
470 organs such as the skin and stomach [10]. In addition, it has indicated that tuning Bmp
471 activity via enhanced epithelial Noggin activity modulates the size and number of the
472 teeth in mice [24]. Herein, we uncovered that natural broadly and persistently distributing
473 pattern of FGF ligands, especially FGF8, in the human tooth germs may be also closely
474 related to its tooth size.

475 **Dental mesenchymal FGF8 signal promotes cell cycle progression from G1- to S-**
476 **stage via enhancing p38 and PI3K-Akt signaling to stimulate proliferation and**
477 **prevent differentiation.**

478 Transduction of FGF signaling is mediated by multiple intracellular pathways,
479 including P38, PI3K/Akt, Erk1/2, and JNK [49]. In our previous study, the similar
480 expression patterns of the indicators in Erk, P38, JNK, and PI3K-Akt pathways in mouse

481 and human tooth germs suggests their conservative regulatory functions during
482 mammalian odontogenesis [43]. P38 has been reported to be involved in control of the cell
483 cycle via the expression changes of P21, P27 and Ccnd3 in mouse skeletal muscle cells
484 [59], Ccnd1 and c-Myc in human dental pulp stem cells [60], and Ccnd1 and P21 in rat
485 mesenchymal stem cells [61], which is also significantly increased in our *Wnt1-Cre;*
486 *R26R*^{Fgf8} mice (Fig. 7). The PI3K-Akt pathway is associated with a variety of cellular
487 functions including cell growth, cell cycle regulation, and cell survival [62]. The increased
488 PI3K-Akt level regulates the proliferation and differentiation of neural progenitor cells
489 by the activation of the cell cycle through the elevation of the Ccnd1 and cyclin E, two
490 cyclins essential for the G1-S transition during organogenesis [63]. Moreover, Akt protein
491 is a central intracellular factor to transduce and integrate multiple extracellular growth
492 factor signals, such as FGF, BMP, and GH/IGF, into a comprehensive signal network to
493 supervise the processes of cell proliferation, growth, and survival [11]. The increased
494 activity of PI3K-Akt pathway caused by augmented FGF8 in the cranial neural crest cell
495 (Fig. 7) further supports its positive function in cell proliferation regulated by cell cycle
496 during tooth development. Erk has been reported to provide a switch-like transition
497 between proliferation and differentiation of muscle progenitors [64], while JNK pathway
498 has been elucidated to play crucial role in negative growth regulation and likely performs
499 a central regulator in both local growth coordination and global growth coordination [4].
500 These two pathways did not show any noticeable alteration in our *Fgf8* transgenic mice,
501 which may attribute to their main function in control of negative growth or balancing cell
502 proliferation and differentiation.

503 Cell growth and division are controlled by the cyclin depend kinases (CDKs) and
504 their binding partners (cyclins) that regulate cell cycle progression through the regulation
505 of the G1-S and G2-M transition. Many cell cycle regulators have been proved to control
506 organ growth, which appears to be generally conserved in *Drosophila* and mammals [(4)].
507 The G1-S phase transition is a rate-limiting step, a known checkpoint between cell growth
508 and cell division, requiring cell cycle regulators to monitor and regulate the progression
509 of the cell cycle [(65)]. The stimulatory effects of cyclins can be offset by CDKs inhibitors
510 (CDKIs) and the repression of CDKIs is also a prerequisite for G1-S transition. Thus
511 merely elevating the level of cyclin D1 is not sufficient to induce cell cycle entry [(66)].
512 Cyclin D1 (Ccnd1) is synthesized rapidly in the G1 phase and accumulates in the nucleus
513 and degraded as the cell enters the S phase [(45)]. P21, known as CDKI1, functions as a
514 regulator of cell cycle progression in G1 and S phase and inhibits all cyclin/CDK
515 complexes, which in turn results in cell cycle arrest and/or apoptosis [(46)]. Enhanced dental
516 mesenchymal FGF8 may promotes cell cycle progression through the regulation of the
517 G1-S transition, which further stimulates cell proliferation and prevents cell
518 differentiation and apoptosis, thereby resulting in prolonged tooth development. In line
519 with this notion, we found that the amount of nuclear Ccnd1^{+} cells is dramatically
520 increased while that of nuclear P21^{+} cells is markedly decreased in the dental
521 mesenchyme at both the early and differentiation stage in *Wnt1-Cre;R26R^{Fgf8}* mice as
522 compared to those in the control (Fig. 8), stating that forcedly enhanced FGF8 in the
523 dental mesenchyme could elevate the level of Ccnd1 and meanwhile suppress the level
524 of p21. Stimulation of Ccnd1 and repression of p21 both constitute the prerequisite for

525 inducing cell cycle entry and thereby promoting the G1-S transition.

526 **FGF8 controls developmental pace in a non-cell-autonomous manner during early**
527 **odontogenesis.**

528 Two latest studies have demonstrated that interspecies differences in developmental
529 tempo are caused by cell-autonomous differences in biochemical reaction speeds instead
530 of differences in signaling, the sequence of genes, or regulatory elements in *in vitro*
531 human and mouse platforms [(67,68)]. Moreover, in *Drosophila*, it is also reported that the
532 *Minute* mutation causes a prolongation of developmental pace and decreased cell division
533 rate in a cell-autonomous way via decreasing the expression of ribosomal proteins and
534 thereby reducing the rate of translation and protein synthesis [(69,70)]. Developmental
535 allochrony regulated in a cell-autonomous manner is highlighted in these studies.
536 However, our findings that the dental mesenchyme resorts to extrinsic signals such as
537 FGF to dominate the developmental tempo as well via tissue interaction in a non-cell-
538 autonomous manner during tooth development are inconsistent with these studies.
539 Additionally, the fact that the oscillation phase shift between Notch and Wnt signaling is
540 critical for the segmentation of presomitic mesoderm cells in multicellular organ
541 development in 2D assays *ex vivo* [(71)] also indicates the pivotal role of secretory signal
542 changes in the regulation of developmental pace. In *Drosophila*, organ growth are
543 orchestrated not only by the growth rate regulated via signaling pathways but also by the
544 growth duration regulated via hormonal signals and organ-autonomous processes
545 controlled by patterning genes and physical force [(4)]. Our heterogenous recombination
546 results provide compelling evidence to support the contribution of extrinsic cues in the

547 developmental tempo of teeth relying on tissue interaction during early development.
548 Thus, we suggest that complicated regulatory networks involved in the developmental
549 pace work both in a cell-autonomous and non-cell-autonomous way to orchestrate the
550 organ morphogenesis, and, particularly, tissue interaction in a non-cell-autonomous way
551 plays a major role during early organogenesis.

552 Tissue bioengineering based on the principle of developmental biology represents a
553 promising approach for repair and regeneration of damaged tissues and organs in the
554 future. However, unmatched development phase between humans and the model animals
555 such as *Drosophila*, zebra fishes, and mice appear to be a major obstacle to acquire
556 knowledge about organ growth control in humans. Uncovering of the molecular
557 mechanism underlying organ growth control in humans is a prerequisite for the realization
558 of replacement therapy in the future. Our study provides important FGF signaling
559 information in tooth developmental process and enlightens our knowledge about the
560 nature of FGF signaling in human tooth growth.

Acknowledgments

This study was supported by the National Natural Science Foundation of China (81870739, 82001002, 81271102, 81771034) and the Natural Science Foundation of Fujian Province (2019J01281, 2020J01180).

References

1. Lloyd AC. The regulation of cell size. Cell. 2013;154(6):1194-205.
2. Promislow DEL, Harvey PH. Living fast and dying young: A comparative analysis of life‐history variation among mammals. J Zool Lond. 1990;220(3):417-37.
3. Swanson EM, Dantzer B. Insulin-like growth factor-1 is associated with life-history variation across Mammalia. Proc Biol Sci. 2014;281(1782):20132458.
4. Gokhale RH, Shingleton AW. Size control: the developmental physiology of body and organ size regulation. Wiley Interdiscip Rev Dev Biol. 2015;4(4):335-56.
5. Barry ER, Morikawa T, Butler BL, Shrestha K, de la Rosa R, Yan KS, et al. Restriction of intestinal stem cell expansion and the regenerative response by YAP. Nature. 2013;493(7430):106-10.
6. Liu M, Zhao S, Wang XP. YAP overexpression affects tooth morphogenesis and enamel knot patterning. J Dent Res. 2014;93(5):469-74.
7. Yu FX, Zhao B, Guan KL. Hippo Pathway in Organ Size Control, Tissue Homeostasis, and Cancer. Cell. 2015;163(4):811-28.
8. Zhang P, Pei C, Wang X, Xiang J, Sun BF, Cheng Y, et al. A Balance of Yki/Sd Activator and E2F1/Sd Repressor Complexes Controls Cell Survival and Affects Organ Size. Dev Cell. 2017;43(5):603-17 e5.
9. Tumaneng K, Russell RC, Guan KL. Organ size control by Hippo and TOR pathways. Curr Biol. 2012;22(9):R368-79.
10. Zaina S, Squire S. The soluble type 2 insulin-like growth factor (IGF-II) receptor reduces organ size by IGF-II-mediated and IGF-II-independent mechanisms. J Biol Chem. 1998;273(44):28610-6.
11. Penzo-Mendez AI, Stanger BZ. Organ-Size Regulation in Mammals. Cold Spring Harb Perspect Biol. 2015;7(9):a019240.
12. Lui JC, Garrison P, Baron J. Regulation of body growth. Curr Opin Pediatr. 2015;27(4):502-10.
13. Zhang YD, Chen Z, Song YQ, Liu C, Chen YP. Making a tooth: growth factors, transcription factors, and stem cells. Cell Res. 2005;15(5):301-16.
14. Polly PD. Gene networks, occlusal clocks, and functional patches: new understanding of pattern and process in the evolution of the dentition. Odontology. 2015;103(2):117-25.
15. Jheon AH, Seidel K, Biehs B, Klein OD. From molecules to mastication: the development and evolution of teeth. Wiley Interdiscip Rev Dev Biol. 2013;2(2):165-82.
16. Salazar-Ciudad I. Tooth patterning and evolution. Curr Opin Genet Dev. 2012;22(6):585-92.
17. Schoenwolf GC BS, Brauer PR, Francis-West PH. Larsen's Human Embryology E-Book. 2014.
18. Rodrigues HG, Renaud S, Charles C, Le Poul Y, Sole F, Aguilar JP, et al. Roles of dental development and adaptation in rodent evolution. Nat Commun. 2013;4:2504.
19. Line SR. Variation of tooth number in mammalian dentition: connecting genetics, development, and evolution. Evol Dev. 2003;5(3):295-304.
20. Edelman GM. Morphoregulation. Dev Dyn. 1992;193(1):2-10.
21. Thesleff I, Sharpe P. Signalling networks regulating dental development. Mech Dev. 1997;67(2):111-23.
22. Jernvall J, Thesleff I. Reiterative signaling and patterning during mammalian tooth morphogenesis. Mech Dev. 2000;92(1):19-29.
23. Tummers M, Thesleff I. The importance of signal pathway modulation in all aspects of tooth development. J Exp Zool B Mol Dev Evol. 2009;312B(4):309-19.

608 24. Plikus MV, Zeichner-David M, Mayer JA, Reyna J, Bringas P, Thewissen JG, et al. Morphoregulation
609 of teeth: modulating the number, size, shape and differentiation by tuning Bmp activity. Evol Dev.
610 2005;7(5):440-57.
611 25. Tapaltsyan V, Charles C, Hu J, Mindell D, Ahituv N, Wilson GM, et al. Identification of novel Fgf
612 enhancers and their role in dental evolution. Evol Dev. 2016;18(1):31-40.
613 26. Thesleff I, Mikkola M. The role of growth factors in tooth development. Int Rev Cytol.
614 2002;217:93-135.
615 27. Tucker A, Sharpe P. The cutting-edge of mammalian development; how the embryo makes teeth.
616 Nat Rev Genet. 2004;5(7):499-508.
617 28. Danielian PS, Muccino D, Rowitch DH, Michael SK, McMahon AP. Modification of gene activity in
618 mouse embryos in utero by a tamoxifen-inducible form of Cre recombinase. Curr Biol.
619 1998;8(24):1323-6.
620 29. Lin C, Yin Y, Bell SM, Veith GM, Chen H, Huh SH, et al. Delineating a conserved genetic cassette
621 promoting outgrowth of body appendages. Plos Genet. 2013;9(1):e1003231.
622 30. Hu X, Lin C, Shen B, Ruan N, Guan Z, Chen Y, et al. Conserved odontogenic potential in embryonic
623 dental tissues. J Dent Res. 2014;93(5):490-5.
624 31. Zhang Y, Wang S, Song Y, Han J, Chai Y, Chen Y. Timing of odontogenic neural crest cell migration
625 and tooth-forming capability in mice. Dev Dyn. 2003;226(4):713-8.
626 32. Song Y, Zhang Z, Yu X, Yan M, Zhang X, Gu S, et al. Application of lentivirus-mediated RNAi in
627 studying gene function in mammalian tooth development. Dev Dyn. 2006;235(5):1334-44.
628 33. Hu X, Xu S, Lin C, Zhang L, Chen Y, Zhang Y. Precise chronology of differentiation of developing
629 human primary dentition. Histochem Cell Biol. 2014;141(2):221-7.
630 34. St Amand TR, Zhang Y, Semina EV, Zhao X, Hu Y, Nguyen L, et al. Antagonistic signals between
631 BMP4 and FGF8 define the expression of Pitx1 and Pitx2 in mouse tooth-forming anlage. Dev Biol.
632 2000;217(2):323-32.
633 35. Dong X, Shen B, Ruan N, Guan Z, Zhang Y, Chen Y, et al. Expression patterns of genes critical for
634 BMP signaling pathway in developing human primary tooth germs. Histochem Cell Biol.
635 2014;142(6):657-65.
636 36. Xiong W, He F, Morikawa Y, Yu X, Zhang Z, Lan Y, et al. Hand2 is required in the epithelium for
637 palatogenesis in mice. Dev Biol. 2009;330(1):131-41.
638 37. Yang G, Yuan G, Ye W, Cho KW, Chen Y. An atypical canonical bone morphogenetic protein (BMP)
639 signaling pathway regulates Msh homeobox 1 (Msx1) expression during odontogenesis. J Biol
640 Chem. 2014;289(45):31492-502.
641 38. Wang B, Li L, Du S, Liu C, Lin X, Chen Y, et al. Induction of human keratinocytes into enamel-
642 secreting ameloblasts. Dev Biol. 2010;344(2):795-9.
643 39. Hu X, Lee JW, Zheng X, Zhang J, Lin X, Song Y, et al. Efficient induction of functional ameloblasts
644 from human keratinocyte stem cells. Stem Cell Res Ther. 2018;9(1):126.
645 40. Hu X, Zhang S, Chen G, Lin C, Huang Z, Chen Y, et al. Expression of SHH signaling molecules in the
646 developing human primary dentition. BMC Dev Biol. 2013;13:11.
647 41. Li CY, Prochazka J, Goodwin AF, Klein OD. Fibroblast growth factor signaling in mammalian tooth
648 development. Odontology. 2014;102(1):1-13.
649 42. Cam Y, Neumann MR, Oliver L, Raulais D, Janet T, Ruch JV. Immunolocalization of acidic and basic
650 fibroblast growth factors during mouse odontogenesis. Int J Dev Biol. 1992;36(3):381-9.
651 43. Huang F, Hu X, Fang C, Liu H, Lin C, Zhang Y, et al. Expression profile of critical genes involved in

652 FGF signaling pathway in the developing human primary dentition. Histochem Cell Biol.
653 2015;144(5):457-69.
654 44. Kettunen P, Thesleff I. Expression and function of FGFs-4, -8, and -9 suggest functional
655 redundancy and repetitive use as epithelial signals during tooth morphogenesis. Dev Dyn.
656 1998;211(3):256-68.
657 45. Baldin V, Lukas J, Marcote MJ, Pagano M, Draetta G. Cyclin D1 is a nuclear protein required for
658 cell cycle progression in G1. Genes Dev. 1993;7(5):812-21.
659 46. Gartel AL, Radhakrishnan SK. Lost in transcription: p21 repression, mechanisms, and
660 consequences. Cancer Res. 2005;65(10):3980-5.
661 47. Cai J, Cho SW, Kim JY, Lee MJ, Cha YG, Jung HS. Patterning the size and number of tooth and its
662 cusps. Dev Biol. 2007;304(2):499-507.
663 48. Jiang TX, Jung HS, Widelitz RB, Chuong CM. Self-organization of periodic patterns by dissociated
664 feather mesenchymal cells and the regulation of size, number and spacing of primordia.
665 Development. 1999;126(22):4997-5009.
666 49. Brewer JR, Mazot P, Soriano P. Genetic insights into the mechanisms of Fgf signaling. Genes Dev.
667 2016;30(7):751-71.
668 50. Lan Y, Jia S, Jiang R. Molecular patterning of the mammalian dentition. Semin Cell Dev Biol.
669 2014;25-26:61-70.
670 51. Abzhanov A, Tzahor E, Lassar AB, Tabin CJ. Dissimilar regulation of cell differentiation in
671 mesencephalic (cranial) and sacral (trunk) neural crest cells in vitro. Development.
672 2003;130(19):4567-79.
673 52. Kratochwil K, Galceran J, Tontsch S, Roth W, Grosschedl R. FGF4, a direct target of LEF1 and Wnt
674 signaling, can rescue the arrest of tooth organogenesis in Lef1(-/-) mice. Genes Dev.
675 2002;16(24):3173-85.
676 53. Kurosaka H, Islam MN, Kuremoto K, Hayano S, Nakamura M, Kawanabe N, et al. Core binding
677 factor beta functions in the maintenance of stem cells and orchestrates continuous proliferation
678 and differentiation in mouse incisors. Stem Cells. 2011;29(11):1792-803.
679 54. Jernvall J, Kettunen P, Karavanova I, Martin LB, Thesleff I. Evidence for the role of the enamel knot
680 as a control center in mammalian tooth cusp formation: non-dividing cells express growth
681 stimulating Fgf-4 gene. Int J Dev Biol. 1994;38(3):463-9.
682 55. Kwon HJ, Li L, Jung HS. Hippo pathway/Yap regulates primary enamel knot and dental cusp
683 patterning in tooth morphogenesis. Cell Tissue Res. 2015;362(2):447-51.
684 56. Song H, Mak KK, Topol L, Yun K, Hu J, Garrett L, et al. Mammalian Mst1 and Mst2 kinases play
685 essential roles in organ size control and tumor suppression. Proc Natl Acad Sci U S A.
686 2010;107(4):1431-6.
687 57. Heallen T, Zhang M, Wang J, Bonilla-Claudio M, Klysik E, Johnson RL, et al. Hippo pathway inhibits
688 Wnt signaling to restrain cardiomyocyte proliferation and heart size. Science.
689 2011;332(6028):458-61.
690 58. Dong J, Feldmann G, Huang J, Wu S, Zhang N, Comerford SA, et al. Elucidation of a universal size-
691 control mechanism in Drosophila and mammals. Cell. 2007;130(6):1120-33.
692 59. Irazoqui AP, Boland RL, Buitrago CG. Actions of 1,25(OH)2-vitamin D3 on the cellular cycle depend
693 on VDR and p38 MAPK in skeletal muscle cells. J Mol Endocrinol. 2014;53(3):331-43.
694 60. Vandomme J, Touil Y, Ostyn P, Olejnik C, Flamenco P, El Machhour R, et al. Insulin-like growth
695 factor 1 receptor and p38 mitogen-activated protein kinase signals inversely regulate signal

696 transducer and activator of transcription 3 activity to control human dental pulp stem cell
697 quiescence, propagation, and differentiation. Stem Cells Dev. 2014;23(8):839-51.
698 61. Stockl S, Bauer RJ, Bosserhoff AK, Gottl C, Grifka J, Grassel S. Sox9 modulates cell survival and
699 adipogenic differentiation of multipotent adult rat mesenchymal stem cells. J Cell Sci.
700 2013;126(Pt 13):2890-902.
701 62. Castellano E, Downward J. RAS Interaction with PI3K: More Than Just Another Effector Pathway.
702 Genes Cancer. 2011;2(3):261-74.
703 63. Xue XJ, Yuan XB. Nestin is essential for mitogen-stimulated proliferation of neural progenitor cells.
704 Mol Cell Neurosci. 2010;45(1):26-36.
705 64. Michailovici I, Harrington HA, Azogui HH, Yahalom-Ronen Y, Plotnikov A, Ching S, et al. Nuclear to
706 cytoplasmic shuttling of ERK promotes differentiation of muscle stem/progenitor cells.
707 Development. 2014;141(13):2611-20.
708 65. Elledge SJ. Cell cycle checkpoints: preventing an identity crisis. Science. 1996;274(5293):1664-72.
709 66. Chambard JC, Lefloch R, Pouyssegur J, Lenormand P. ERK implication in cell cycle regulation.
710 Biochim Biophys Acta. 2007;1773(8):1299-310.
711 67. Rayon T, Stamataki D, Perez-Carrasco R, Garcia-Perez L, Barrington C, Melchionda M, et al.
712 Species-specific pace of development is associated with differences in protein stability. Science.
713 2020;369(6510).
714 68. Matsuda M, Hayashi H, Garcia-Ojalvo J, Yoshioka-Kobayashi K, Kageyama R, Yamanaka Y, et al.
715 Species-specific segmentation clock periods are due to differential biochemical reaction speeds.
716 Science. 2020;369(6510):1450-5.
717 69. Saebøe-Larssen S, Lyamouri M, Merriam J, Oksvold MP, Lambertsson A. Ribosomal protein
718 insufficiency and the minute syndrome in Drosophila: a dose-response relationship. Genetics.
719 1998;148(3):1215-24.
720 70. Morata G, Ripoll P. Minutes: mutants of drosophila autonomously affecting cell division rate. Dev
721 Biol. 1975;42(2):211-21.
722 71. Sonnen KF, Lauschke VM, Uraji J, Falk HJ, Petersen Y, Funk MC, et al. Modulation of Phase Shift
723 between Wnt and Notch Signaling Oscillations Controls Mesoderm Segmentation. Cell.
724 2018;172(5):1079-90 e12.

725 # Tables

726 **Table. 1 Ratio of tooth formation in different types of tissue recombinants.**

Type of Recombinant		No. of Recombinant	No. of Tooth Formation	Ratio (%)
Epithelium	Mesenchyme			
mde	mdm	28	28	100
mde	hdm	78	76	97.4
hde	mdm	27	24	88.9

727 Abbreviations: mdm, E13.5 mouse dental mesenchyme; hdm, bell-stage human dental mesenchyme
728 (14-16 weeks of gestation); mde, E13.5 mouse dental epithelium; hde, bell-stage human dental
729 epithelium (14-16 weeks of gestation).

730 # Figure legends

731 **Fig. 1. Heterogenous recombination of human and mouse embryonic dental tissues**
732 **reveals the dominant role of the dental mesenchyme in the control of tooth**
733 **developmental pace. A-C**: Azan dichromic staining (stains dentin blue and enamel red)
734 of recombinants of E13.5 mouse dental epithelium and bell-stage human dental
735 mesenchyme cultured under the kidney capsule for 3 weeks (**A**), 4 weeks (**B**), 8 weeks
736 (**C**). Note that no deposition of dentin and enamel was seen in the chimeric tooth germs
737 until 4 weeks in subrenal culture. **D-F**: Azan dichromic staining of recombinants of E13.5
738 mouse dental epithelium and E13.5 mouse dental mesenchyme cultured under the kidney
739 capsule for 6 days (**D**), 7 days (**E**), and 8 days (**F**). Note that the deposition of dentin and
740 enamel was not seen until 7 and 8 days, respectively, in subrenal culture. **G-I**: Azan
741 dichromic staining of recombinants of bell-stage human dental epithelium and E13.5
742 mouse dental mesenchyme cultured under the kidney capsule for 7 days (**G**), 9 days (**H**),
743 and 10 days (**I**). Note that the deposition of dentin and enamel was not seen until 9 and
744 10 days, respectively, in subrenal culture. **J-R**: The expression of ameloblastin and
745 MMP20 in recombinants of E13.5 mouse dental epithelium and bell-stage human dental
746 mesenchyme cultured under the kidney capsule for 3 weeks (**J**), 4 weeks (**K** and **L**), in
747 recombinants of E13.5 mouse dental epithelium and mouse dental mesenchyme for 6 days
748 (**M**), 7 days (**N** and **O**), and in recombinants of bell-stage human dental epithelium and
749 mouse dental mesenchyme for 7 days (**P**) and 9 days (**Q** and **R**). hdm, human dental
750 mesenchyme; hde, human dental epithelium; mdm, mouse dental mesenchyme; mde,
751 mouse dental epithelium; hod, human odontoblasts; mod, mouse odontoblasts; mam,

752 mouse ameloblasts; d, dentin; e, enamel. Scale bar = 50 μm.

753

754 **Fig. 2. FGF signaling is involved in the regulation of tooth developmental pace. A-C**:
755 Immunostaining showing the expression of pSmad1/5/8 (**A**), K-Ras (**B**), and β-catenin
756 (**C**) in recombinants of mouse dental epithelium and mouse dental mesenchyme cultured
757 under the kidney capsule for 7 days. **D-F**: Immunostaining showing the expression of
758 pSmad1/5/8 (**D**), K-Ras (**E**), and β-catenin (**F**) in recombinants of mouse dental
759 epithelium and human dental mesenchyme cultured under the kidney capsule for 4 weeks.
760 **G**: Human 1st premolar germs of 16th week gestation were transplanted under the kidney
761 capsule and cultured in the absence or presence of SU5402 for 2 days. Note the decreased
762 expression of pErk1/2 and pPDK1 in the presence of SU5402. **H-I**: Human 1st premolar
763 germs of 16th week gestation were transplanted under the kidney capsule and cultured in
764 the absence (**H**) or presence (**I**) of SU5402 for 1 week. Note the accelerated detinogenesis
765 with the appearance of dentin (**I**, red arrow) in the presence of SU5402. **J-L**:
766 Immunohistochemical staining showing the expression of FGF4 (**J**), FGF8 (**K**), and
767 FGF9 (**L**) in recombinants of mouse dental epithelium and human dental mesenchyme
768 cultured under the kidney capsule for 4 weeks and the expression of FGF8 (insert in **K**)
769 in recombinants of human dental epithelium and mouse dental mesenchyme cultured
770 under the kidney capsule for 10 days. mam, mouse ameloblasts; mod, mouse odontoblasts;
771 hod, human odontoblasts; am, ameloblasts; od, odontoblasts; iee, inner enamel epithelium;
772 sr, stellate reticulum; dm, dental mesenchyme; d, dentin; pre-d, predentin. Scale bar = 25
773 μm.

774

775 **Fig. 3. Augmented FGF8 signaling in the mouse dental mesenchyme delays tooth**
776 **development and increases cell proliferation.** **A**, **B**: Azan dichromic staining of
777 recombinants of E13.5 mouse dental epithelium and re-aggregate of dental mesenchymal
778 cells infected with control LV-*eGFP* (**A**) or LV-*Fgf8-eGFP* (**B**) cultured under the kidney
779 capsule for 6 days (insert in **A**), 7 days, and 9 days (insert in **B**). **C**, **D**: Immunostaining
780 showing the expression of Ki67 in recombinants of E13.5 mouse dental epithelium and
781 re-aggregate of dental mesenchymal cells infected with control LV-*eGFP* (**C**) or LV-*Fgf8-*
782 *eGFP* (**D**) cultured under the kidney capsule for 7 days. **E**: Comparison of Ki67-positive
783 cells in the dental mesenchyme and dental epithelium of the recombinants. Standard
784 deviation values were shown as error bars, and ** indicates $p < 0.01$, $n = 6$/group. **F**: GFP
785 staining of recombinants of E13.5 mouse dental epithelium and re-aggregate of dental
786 mesenchymal cells infected with control LV-*eGFP* cultured under the kidney capsule for
787 11 days. dm, dental mesenchyme; dp, dental pulp; am, ameloblasts; sr, stellate reticulum;
788 od, odontoblasts; d, dentin; Epi, epithelium; Mes, mesenchyme. Scale bar = 25 μm.

789

790 **Fig. 4. Delayed tooth development in early molar germs of *Wnt1-Cre;R26R^{Fgf8}* mice.**
791 **A-H:** H&E staining showing the morphology of maxillary and mandibular molar in E13.5
792 wild-type (**A**,**C**) and mutant (**B**,**D**) embryos and in E14.5 wild-type (**E**,**G**) and mutant
793 (**F**,**H**) embryos. de, dental epithelium; dm, dental mesenchyme. Scale bar = 50 μm.

794

795 **Fig. 5. Grafts of *Wnt1-Cre;R26R^{Fgf8}* molar germs exhibit delayed tooth development**

796 **and enlarged tooth size. A-H**: Azan dichromic staining of E11.5 wild-type and mutant
797 maxillary molar germs cultured under the kidney capsule for 8 days (**A**,**B**), 9 days (**C**,**D**),
798 10 days (**E**,**F**), 12 days (insert in **F**), and 18 days (**G**,**H**). Azan dichromic staining of E11.5
799 mutant mandibular molar germs cultured under the kidney capsule for 9 days (insert in
800 **D**). **I-L**: Immunostaining showing the expression of DSP (**I,J**) and Ameloblastin (**K,L**) in
801 E11.5 wild-type and mutant molar grafts cultured under the kidney capsule for 9 days. **M**,
802 **N**: Representative Micro-CT images of E11.5 wild-type (**M**) and mutant molar germs (**N**)
803 cultured under the kidney capsule for 3 months. **O**: Comparison of the height and width
804 of the tooth crown between wild-type and mutant mineralized teeth cultured under the
805 kidney capsule for 3 months. Standard deviation values were shown as error bars. ns
806 indicates $p > 0.05$, and ** indicates $p < 0.01$, $n = 7$ and 11/group in **O**. de, dental
807 epithelium; dm, dental mesenchyme; am, ameloblasts; od, odontoblasts; d, dentin; e,
808 enamel. Scale bar: A-H, I-L = 50 μm; M and N = 500 μm.
809
810 **Fig. 6. Ectopically activated dental mesenchymal FGF8 signaling stimulates cell**
811 **proliferation and prevents cell apoptosis during odontogenesis. A-F**: Immunostaining
812 showing the Ki67 positive cells in E13.5 wild-type (**A**) and mutant (**D**) molar germs and
813 in the grafts of E11.5 wild-type and mutant molar germ cultured under the kidney
814 capsule for 9 days (**B**,**E**) and 18 days (**C**,**F**). **G-J**: Immunostaining showing the expression
815 of Caspase3 in the grafts of E11.5 wild-type (**G**, boxed area is magnified in **H**) and mutant
816 (**I**, boxed area is magnified in **J**) molar germ cultured under the kidney capsule for 18
817 days. Note the absence of Caspase3 expression in the dental mesenchyme (red asterisk)

818 excepting odontoblasts in mutant grafts. **K-M**: The percentage of Ki67 positive cells in
819 the dental mesenchyme of wild-type and mutant E13.5 tooth germs (**K**) and tooth grafts
820 cultured under the kidney capsule for 9 days (**I**) and 18 days (**M**), n = 3/group, * indicates
821 $p < 0.05$. Standard deviation values were shown as error bars. am, ameloblasts; od,
822 odontoblasts; d, dentin; e, enamel. Scale bar = 100 μm.

823

824 **Fig. 7. Ectopically activated dental mesenchymal FGF8 signaling is transduced via**
825 **p38 and PI3K-Akt intracellular pathways. A-D**: Immunostaining showing the
826 expression of pErk1/2 in E13.5 wild-type (**A**) and mutant (**B**) molar germs and in E11.5
827 wild-type (**C**) and mutant (**D**) molar germs cultured under the kidney capsule for 9 days.
828 **E-H**: Immunostaining showing the expression of pJNK in E13.5 wild-types (**E**) and
829 mutants (**F**) molar germs and in E11.5 wild-type (**G**) and mutant (**H**) molar germs cultured
830 under the kidney capsule for 9 days. **I-L**: Immunostaining showing the expression of pP38
831 in E13.5 wild-type (**I**) and mutant (**J**) molar germs and in E11.5 wild-type (**K**) and mutant
832 (**L**) cultured under the kidney capsule for 9 days. **M-P**: Immunostaining showing the
833 expression of pAkt1 in E13.5 wild-types (**M**) and mutants (**N**) molar germs and in E11.5
834 wild-type (**O**) and mutant (**P**) molar germs cultured under the kidney capsule for 9 days.
835 **Q**: Western-blotting of pErk1/2, pP38, pJNK, and pAKT1 expressed in E13.5 wild-type
836 and mutant molar germs. **R**: Quantification of immunoblotting data in **Q**. n = 3/group. *
837 indicates $p < 0.05$. Standard deviation values were shown as error bars. de, dental
838 epithelium; dm, dental mesenchyme; am, ameloblasts; od, odontoblasts. Scale bar = 25
839 μm.

840

841 **Fig. 8. Enhanced dental mesenchymal FGF8 signaling increases the level of nuclear**
842 **Ccnd1 and decreases the level of nuclear p21.** Immunostaining showing the
843 colocalization of Ccnd1 and P21 in E13.5 wild-type (**A-D**) and mutant (**E-H**) molar germs
844 and E11.5 wild-type (**I-L**) and mutant (**M-P**) molar germs cultured under the kidney
845 capsule for 9 days. Boxed areas in (**C**), (**G**), (**K**), and (**O**) are magnified in (**D**), (**H**), (**L**),
846 and (**P**), respectively. Note the significantly increased proportion of Ccnd1-positive cells
847 (white arrow) and the shift of P21 from the nuclei to the cytoplasm (yellow arrow) in the
848 mutant dental mesenchyme (**P**) as compared with wild-type ones (**L**). de, dental
849 epithelium; dm, dental mesenchyme; am, ameloblasts; od, odontoblasts. Scale bar: A-N,
850 P-S = 50 μm; O, T = 25 μm.

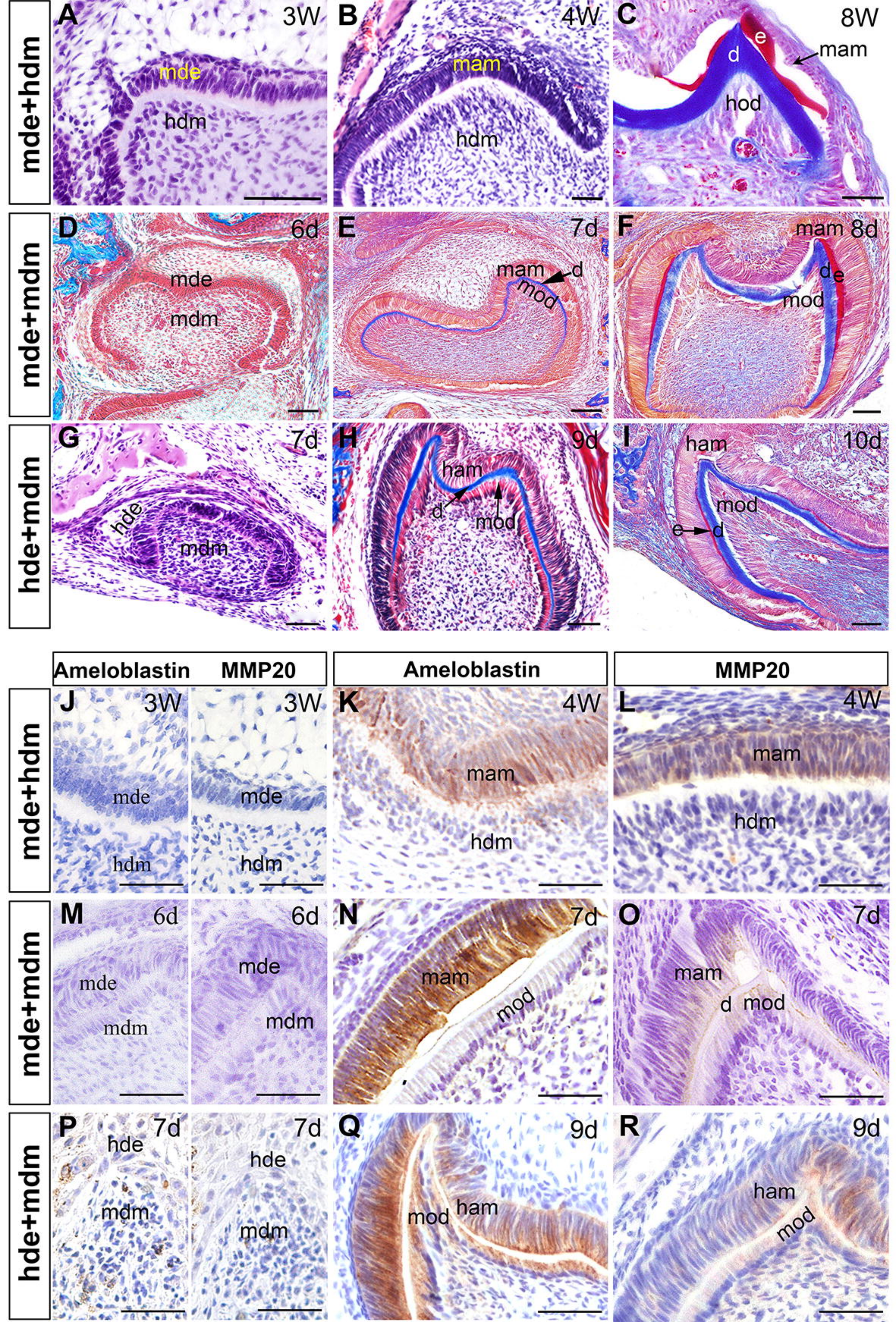
mde+hdm
A
3W
mde
hdm
B
4W
mam
hdm
C
8W
e
d
mam
hod
mde+mdm
D
6d
mde
mdm
E
7d
mam
d
mod
F
mam 8d
de
mod
hde+mdm
G
7d
hde
mdm
H
9d
ham
d
mod
I
ham
10d
mod
e
d
Ameloblastin
MMP20
Ameloblastin
MMP20
mde+hdm
J
3W
mde
hdm
3W
mde
hdm
K
4W
mam
hdm
L
4W
mam
hdm
mde+mdm
M
6d
mde
mdm
6d
mde
mdm
N
7d
mam
mod
O
7d
mam
d
mod
hde+mdm
P
7d
hde
mdm
7d
hde
mdm
Q
9d
mod
ham
R
9d
ham
mod

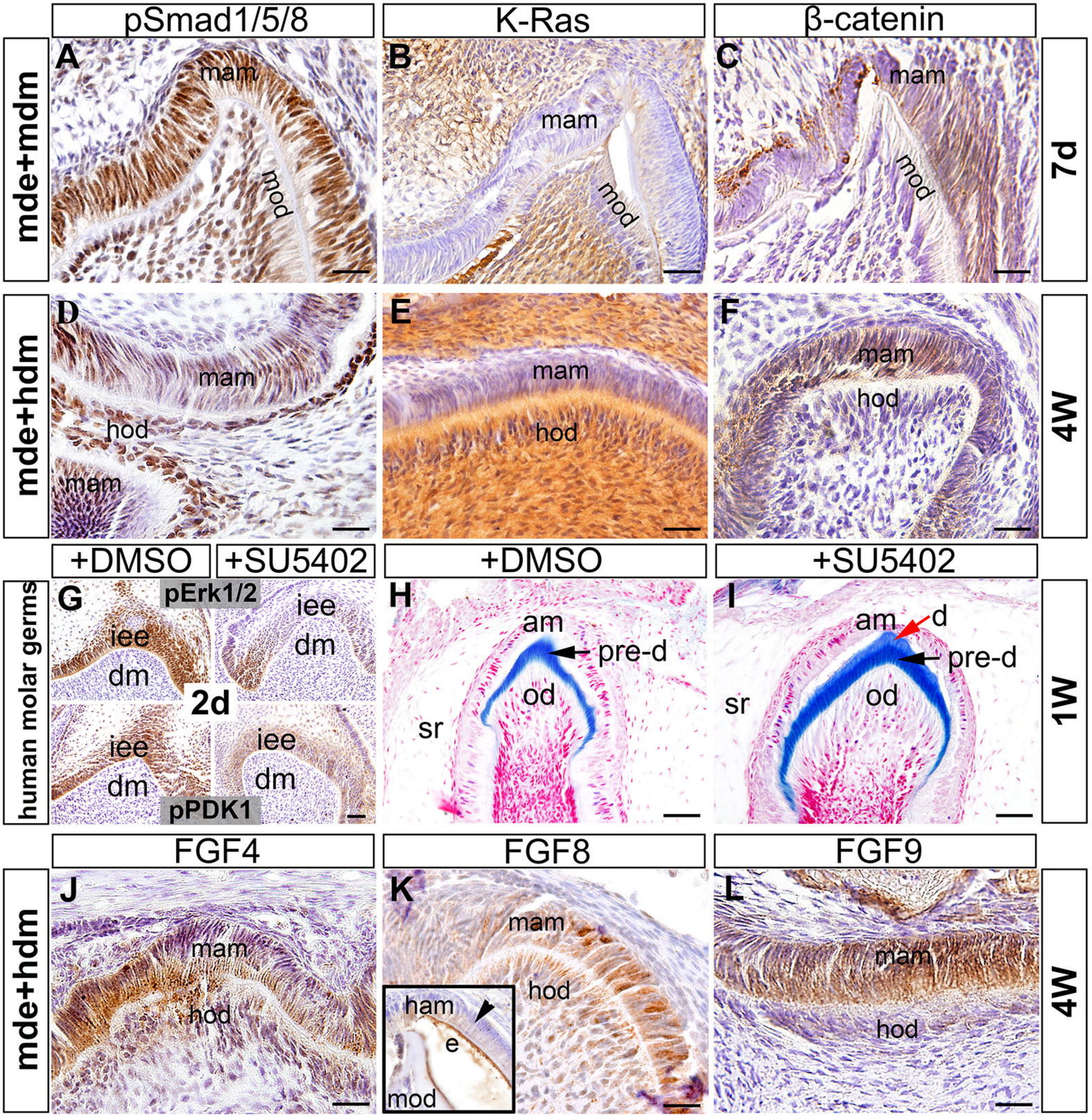
pSmad1/5/8
K-Ras
β-catenin
mde+mdm
7d
A
mam
mod
B
mam
mod
C
mam
mod
mde+hdm
4W
D
mam
hod
mam
E
mam
hod
F
mam
hod
+DMSO
+SU5402
+DMSO
+SU5402
human molar germs
1W
G
pErk1/2
iee
dm
iee
dm
2d
iee
dm
iee
dm
pPDK1
H
am
pre-d
od
sr
I
am
d
pre-d
sr
od
FGF4
FGF8
FGF9
mde+hdm
4W
J
mam
hod
K
mam
hod
ham
e
mod
L
mam
hod

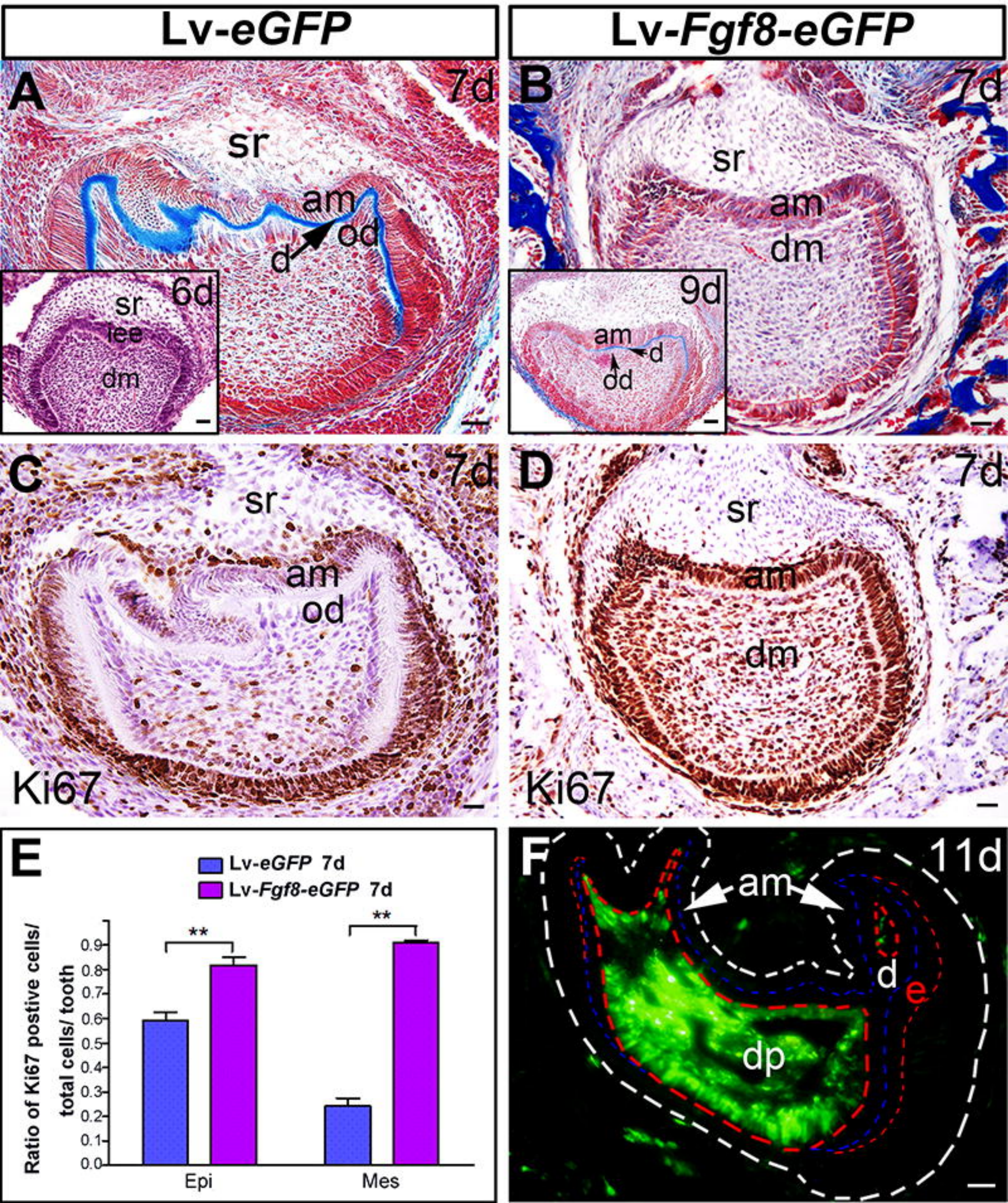
Lv-eGFP
Lv-Fgf8-eGFP
A
7d
sr
am
od
d
6d
sr
iee
dm
B
7d
sr
am
dm
9d
am
d
od
C
7d
sr
am
od
Ki67
D
7d
sr
am
dm
Ki67
E
Lv-eGFP 7d
Lv-Fgf8-eGFP 7d
Ratio of Ki67 postive cells/ total cells/ tooth
0.0
0.1
0.2
0.3
0.4
0.5
0.6
0.7
0.8
0.9
**
**
Epi
Mes
F
11d
am
d
e
dp

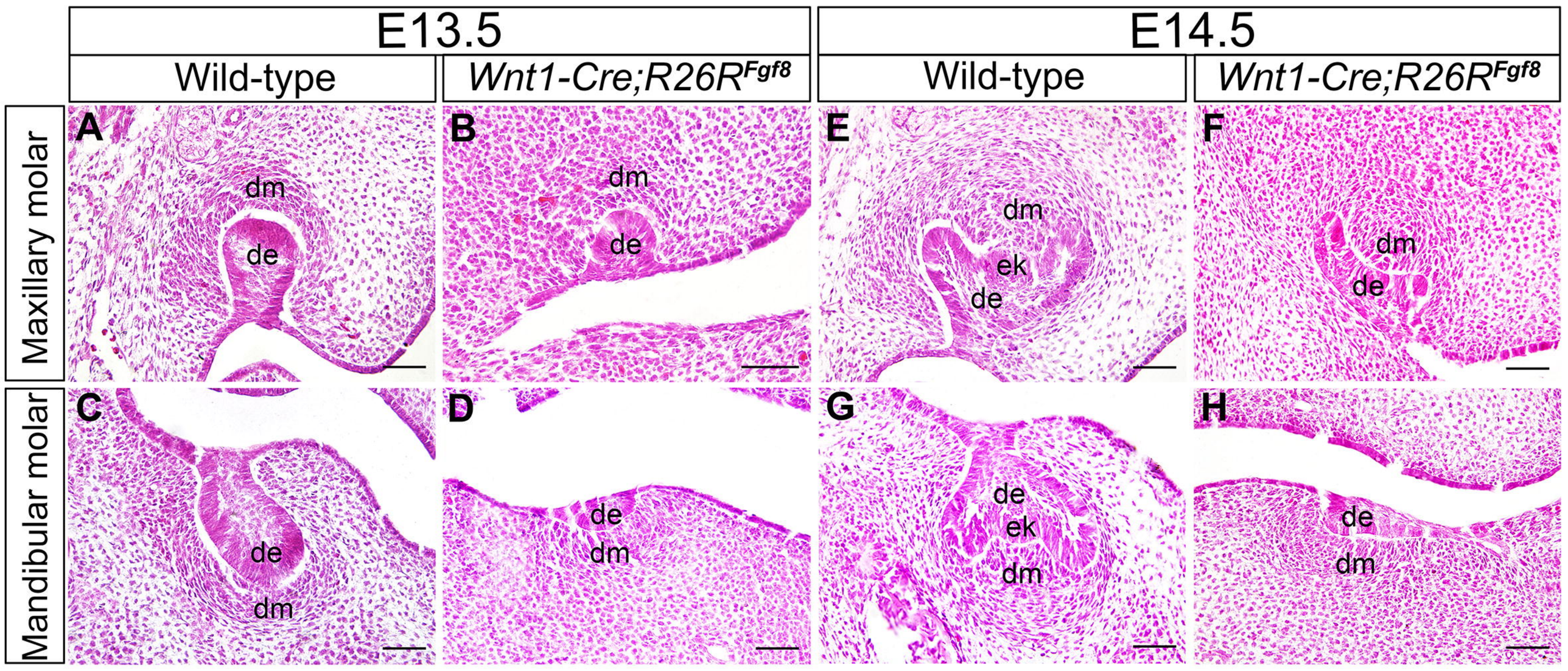
E13.5
E14.5
Wild-type
Wnt1-Cre;R26RFgf8
Wild-type
Wnt1-Cre;R26RFgf8
Maxillary molar
Mandibular molar
A
B
C
D
E
F
G
H
dm
de
ek

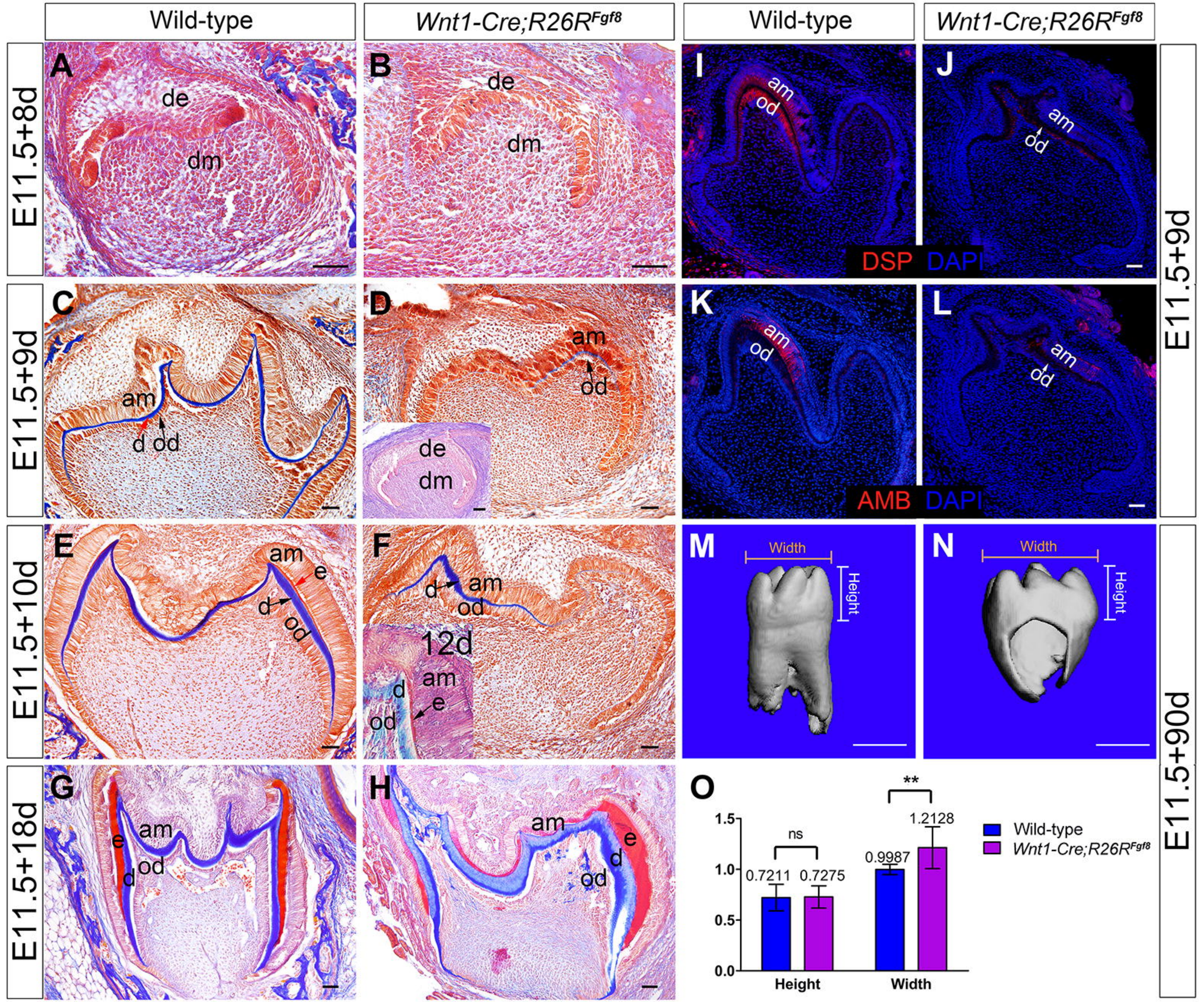
Wild-type
Wnt1-Cre;R26R^Fgf8
Wild-type
Wnt1-Cre;R26R^Fgf8
E11.5+8d
E11.5+9d
E11.5+10d
E11.5+18d
E11.5+90d
A
B
C
D
E
F
G
H
I
J
K
L
M
N
O
de
dm
am
od
d
e
12d
DSP
DAPI
AMB
Width
Height
ns
**
0.7211
0.7275
0.9987
1.2128
1.5
1.0
0.5
0.0
Height
Width
Wild-type
Wnt1-Cre;R26R^Fgf8

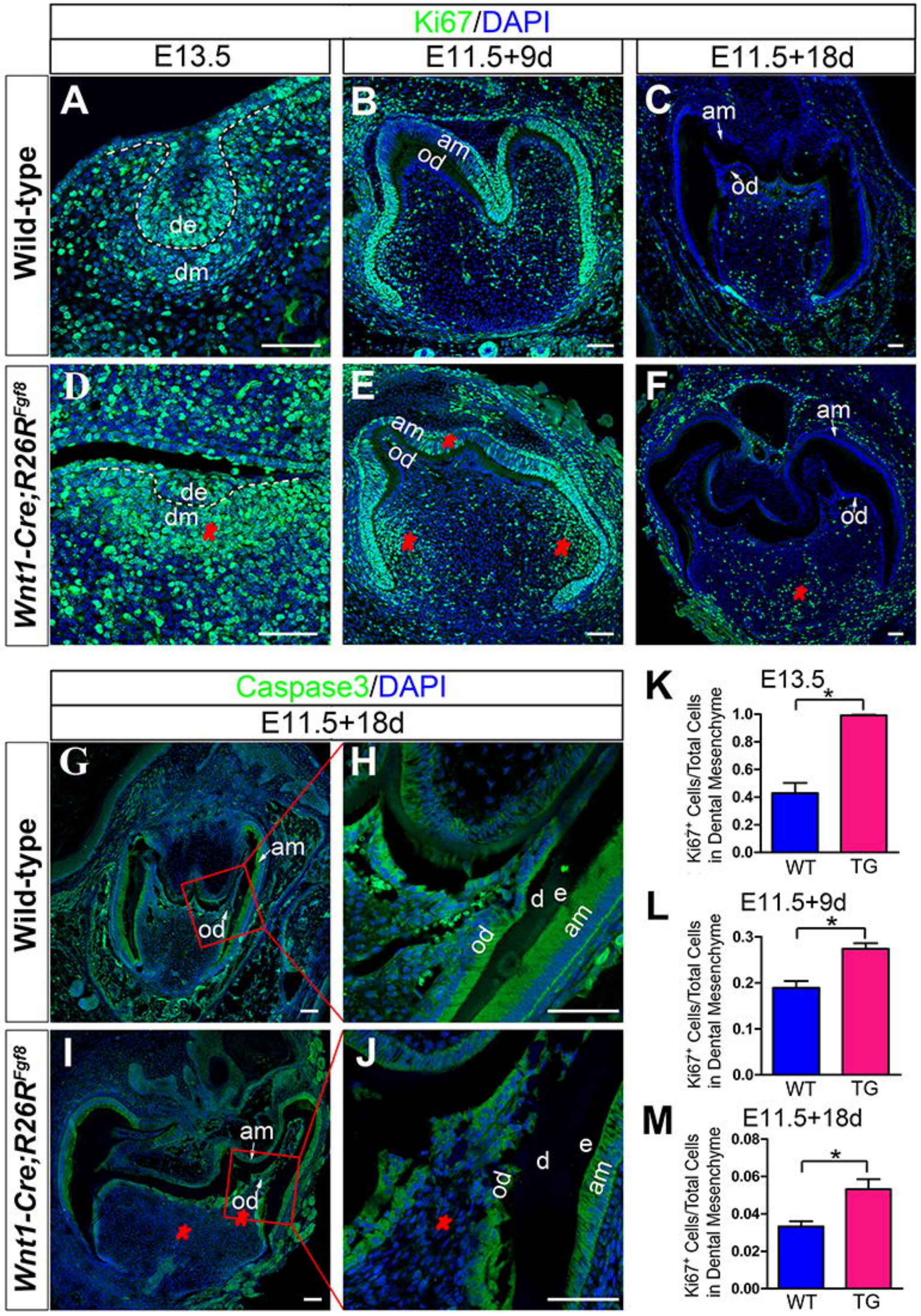
Ki67/DAPI
E13.5
E11.5+9d
E11.5+18d
Wild-type
Wnt1-Cre;R26R^Fgf8
A
B
C
D
E
F
de
dm
am
od
Caspase3/DAPI
E11.5+18d
G
H
I
J
d
e
K
E13.5
L
E11.5+9d
M
E11.5+18d
Ki67+ Cells/Total Cells in Dental Mesenchyme
WT
TG
*

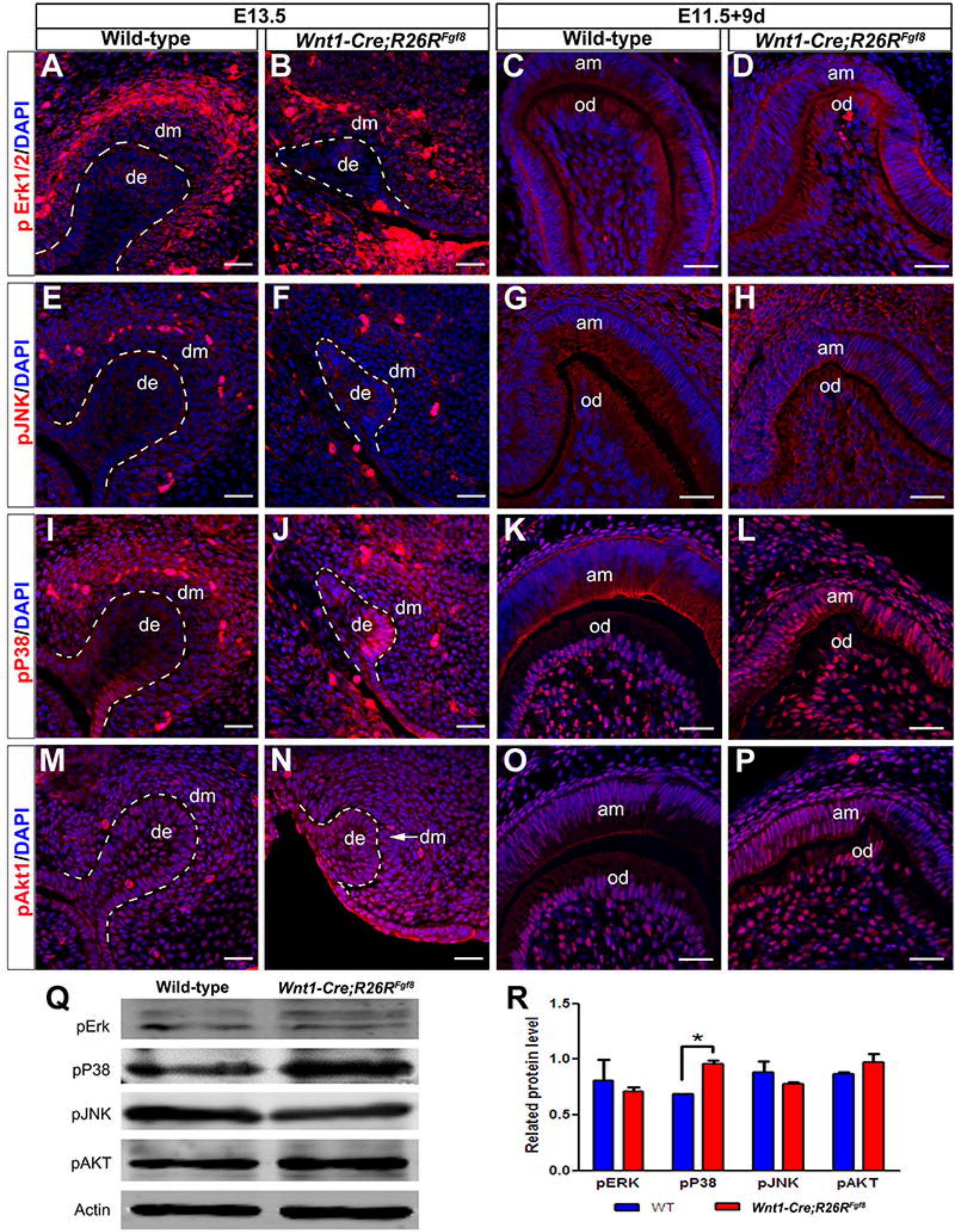
E13.5
E11.5+9d
Wild-type
Wnt1-Cre;R26R^Fgf8
Wild-type
Wnt1-Cre;R26R^Fgf8
p Erk1/2/DAPI
pJNK/DAPI
pP38/DAPI
pAkt1/DAPI
A
B
C
D
E
F
G
H
I
J
K
L
M
N
O
P
dm
de
am
od
Q
Wild-type
Wnt1-Cre;R26R^Fgf8
pErk
pP38
pJNK
pAKT
Actin
R
Related protein level
1.5
1.0
0.5
0.0
*
pERK
pP38
pJNK
pAKT
WT
Wnt1-Cre;R26R^Fgf8

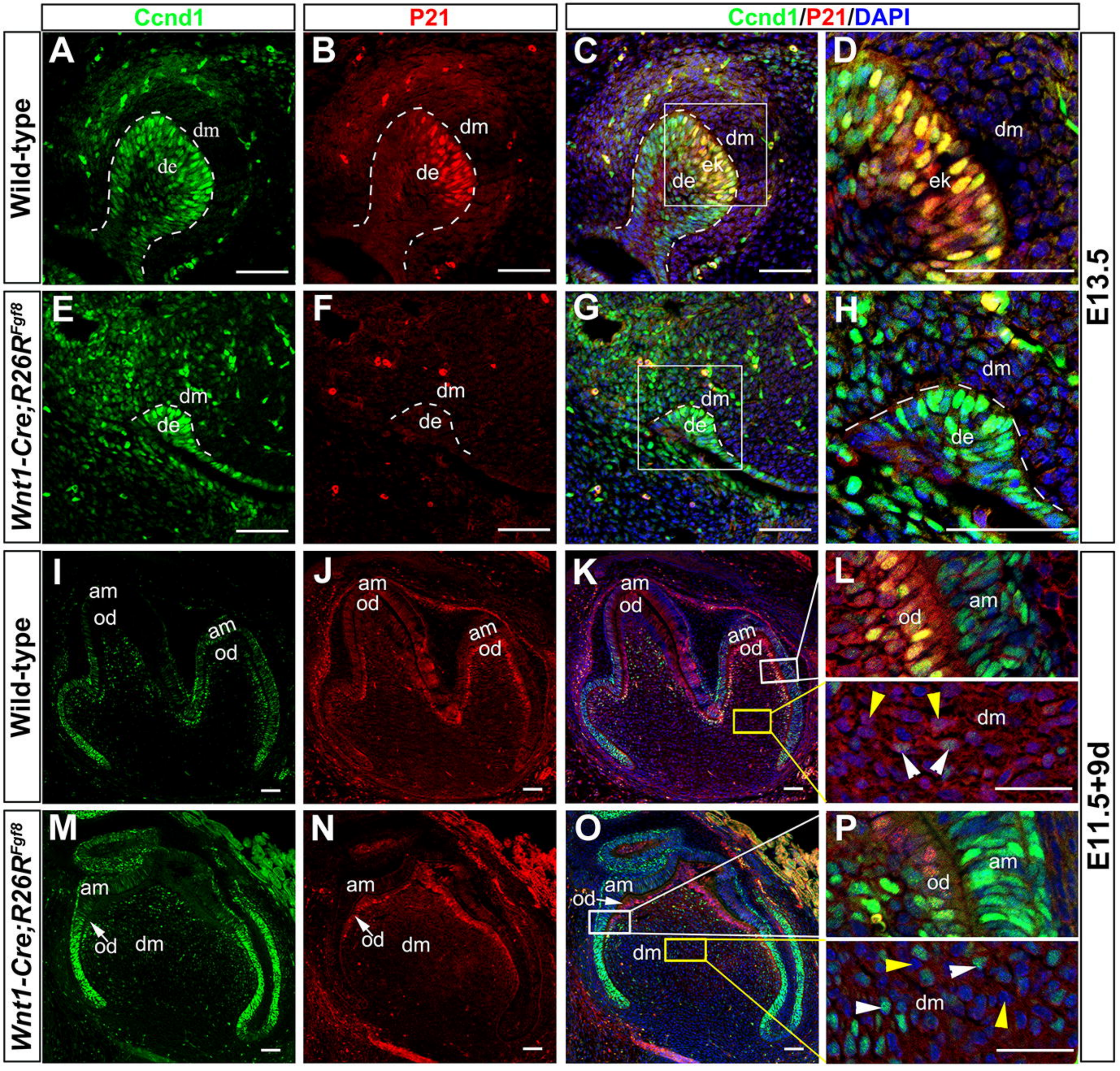
Ccnd1
P21
Ccnd1/P21/DAPI
Wild-type
Wnt1-Cre;R26R^Fgf8
E13.5
E11.5+9d
A
B
C
D
E
F
G
H
I
J
K
L
M
N
O
P
dm
de
ek
am
od